MLF Experimental Report	提出日 Date of Report March, 2010
課題番号 Project No. 2009B0004 実験課題名 Title of experiment In situ neutron diffraction study for Fe-based shape memory materials 実験責任者名 Name of principal investigator Hiroyuki Y. Yasuda 所属 Affiliation Osaka University	装置責任者 Name of responsible person Kazuya Aizawa, Stefanus Harjo 装置名 Name of Instrument/（BL No.） BL19 実施日 Date of Experiment January, 27, 28, 30, 2010

試料、実験方法、利用の結果得られた主なデータ、考察、結論等を、記述して下さい。（適宜、図表添付のこと）
Please report your samples, experimental method and results, discussion and conclusions. Please add figures and tables for better explanation.

1. 試料 Name of sample(s) and chemical formula, or compositions including physical form.

(A) Fe-Al single crystals and polycrystals
- ・Fe-23at%Al single crystals with different loading axes
- ・Fe-23at%Al polycrystals

(B) Fe-Ga single crystals and polycrystals
- ・Fe-24at%Ga single crystals and polycrystals
- ・Fe-28at%Ga polycrystals

(C) Co-50at%Zr polycrystals

2. 実験方法及び結果（実験がうまくいかなかった場合、その理由を記述してください。）
Experimental method and results. If you failed to conduct experiment as planned, please describe reasons.

In situ neutron diffraction study was carried out to examine deformation behavior of Fe-Al and Fe-Ga shape memory materials with the $D0_3$ superlattice structure. We also studied the deformation behavior of CoZr alloys which is a potential candidate for hydrogen permeable film.

A. in situ neutron diffraction study for Fe-Al alloys

Fe-23at%Al single crystals were tensile deformed with different orientations at room temperature and in situ neutron diffraction was taken by engineering diffractometer TAKUMI (BL19). No diffraction peak corresponding to martensitic transformation could be detected during loading-unloading cycle. In contrast, the position and FWHM of the neutron diffraction peaks were consistent with superelasticity based on dislocation motion, schematically shown in Fig. 1. Figure 2 shows change in (420) peak of Fe-23at%Al single crystals with nominal strain (ε). The angle between [420] direction and loading axis is 6.4°. At the onset of plastic deformation, the (420) peak shifts to higher lattice

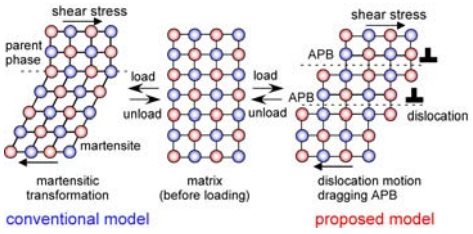

Fig.1 Superelasticity based on dislocation motion.

2. 実験方法及び結果（つづき） Experimental method and results (continued)

spacings due to tensile elastic strain. At 2% ≤ ε ≤ 5%, peak broadening occurs corresponding to the accumulation of dislocations. At the initial stage of unloading, the (420) peak shift to lower plane spacings because of the release of elastic strain. The (420) peak becomes sharp by further unloading since the dislocations disappear. After unloading, the position and FWHM of the (420) peaks is almost the same as those before loading. In situ neutron diffraction study was also carried out for Fe-23at%Al polycrystals compressed to 5 % at room temperature. Even after deformation to 5 %, all the diffraction peaks could be indexed with respect to the $D0_3$ structure. This also suggests that the superelastic deformation in Fe-23at%Al alloys is not based on martensitic transformation but dislocation motion shown in Fig. 1.

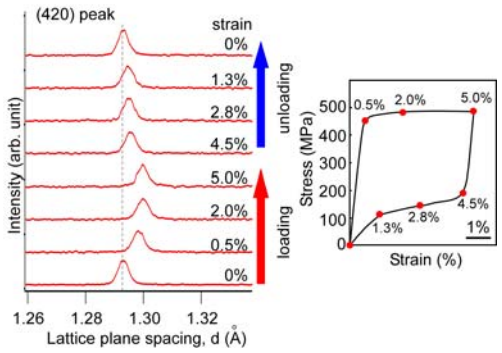

Fig.2 Variation in (420) peak with tensile strain in Fe-23at%Al single crystal pulled at room temperature.

<u>B. in situ neutron diffraction study for Fe-Ga alloys</u>

Fe-Ga alloys solutionized at 900 ℃ exhibited superelasticity partly based on martensitic transformation. Figure 3 shows neutron diffraction profiles of Fe-24at%Ga polycrystals compressed to 1 % at room temperature. At ε=1 %, a small new peak is observed in the vicinity of (220) peak. We also observed the new peak in the diffraction profiles in Fe-28at%Ga polycrystals subjected to compression. Thus, one can conclude that reversible martensitic transformation as well as dislocation motion during loading-unloading cycle contributes to the superelasticity in Fe-Ga alloys.

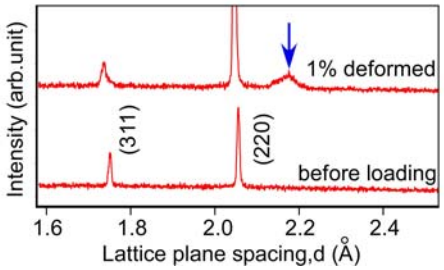

Fig.3 Neutron diffraction profiles of Fe-24at%Ga polycrystals compressed at room temperature.

<u>C. in situ neutron diffraction study for CoZr alloys</u>

B2-ordered CoZr grains of which loading axis is [001] cannot be plastically deformed since the slip system of CoZr is {110}<001>. Thus, the [001]-oriented grains behave as a hard-grain in the polycrystals which may lead to strong stress/strain partitioning. Figure 4 shows variation in spacing of (200), (220) and (111) planes with applied stress during tensile deformation of CoZr polycrystals. Note that the planes were almost perpendicular to the tensile axis. As shown in Fig. 4, CoZr polycrystals demonstrate strong stress/strain partitioning. At the initial stage of tensile deformation, the lattice spacing of (200), (220) and (111) planes increases with increasing applied stress. On the other hand, the spacing of (220) and (111) planes tends to be saturated above the yield stress (150 MPa). In contrast, the (200) plane spacing rises monotonically even after the yielding. Thus, strong stress/strain partitioning was confirmed to occur in CoZr alloys by in situ neutron diffraction study.

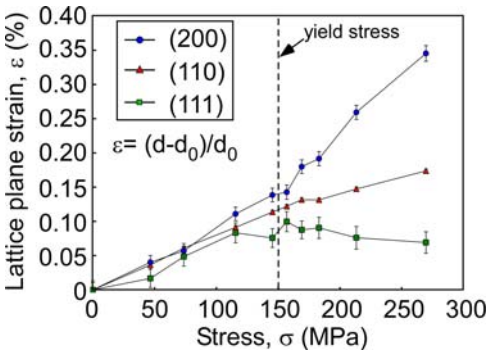

Fig.4 Variation in lattice plane strain with applied stress in CoZr polycrystals during tensile loading.